On Power Quality of Variable-Speed Constant-Frequency Aircraft Electric Power Systems

Ahmad Eid, *Student Member, IEEE*, Hassan El-Kishky, *Senior Member, IEEE*, Mazen Abdel-Salam, *Fellow, IEEE*, and Mohamed T. El-Mohandes, *Member, IEEE*

***Abstract*—In this paper, a comprehensive model of the variable-speed constant-frequency aircraft electric power system is developed to study the performance characteristics of the system and, in particular, the system power quality over a frequency range of operation of 400 Hz to 800 Hz. A fully controlled active power filter is designed to regulate the load terminal voltage, eliminate harmonics, correct supply power factor, and minimize the effect of unbalanced loads. The control algorithm for the active power filter (APF) is based on the perfect harmonic cancellation method which provides a three-phase reference supply current in phase with its positive-sequence fundamental voltage. The proposed APF is integrated into the model of a 90-kVA advanced aircraft electric power system under VSCF operation. The performance characteristics of the system are studied with the frequency of the generator's output voltage varied from 400 Hz to 800 Hz under different loading conditions. Several case studies are presented including dc loads as well as passive and dynamic ac loads. The power quality characteristics of the studied aircraft electric power system with the proposed active filter are shown to be in compliance with the most recent military aircraft electrical standards MIL-STD-704F as well as with the IEEE Std. 519.**

***Index Terms*—Aircraft power system, active power filter (APF), total harmonic distortion (THD), variable-speed constant-frequency (VSCF).**

I. Introduction

THE architecture of a conventional civil aircraft consists of a combination of systems: mechanical, pneumatic, hydraulic, and electrical systems. These systems have several drawbacks, such as low efficiency and difficulty in detecting leaks in a pneumatic system; the use of gearboxes in a mechanical system; heavy, inflexible piping; and the potential leakage of dangerous and corrosive fluids for the hydraulic system [1]. The concept of the "all-electric aircraft" and the "more electric aircraft" (MEA) have been introduced to overcome some of the drawbacks found in conventional architectures and bring more attractive advantages, such as improved fuel consumption, and lower maintenance and operation costs [1]–[3]. The electrical power does not require a heavy infrastructure and is very flexible. However, it still suffers some drawbacks, such as low-power density compared to hydraulic power and may result in a higher risk of fire in case of a short circuit.

The constant-speed drive (CSD) generating system found onboard many aircrafts is comprised of a three-stage regulated synchronous generator, the output frequency of which is maintained constant by means of a hydro-mechanical CSD connecting it to the engine via a gearbox. A reduction in the weight of the system is brought about by a combination of the drive and the generator integrated into a single unit, thereby providing the integrated drive generator (IDG) [3], [4]. However, continuing developments in power electronics and microprocessor technology have led to the dc-link variable-speed constant-frequency (VSCF) generating system [5], [6], becoming a viable alternative to the CSD and IDG systems. The VSCF electrical system is more flexible compared to the CSD/IDG systems since its components can be distributed throughout the aircraft, in contrast to the CSD/IDG mechanical system in which they must inevitably be located close to the engine.

In this paper, a complete model for the VSCF advanced aircraft electric power system (EPS) is developed. A fully controlled APF is designed to regulate the load terminal voltage, eliminate harmonics, correct supply power factor, and to minimize the effect of unbalanced loads. A three-phase-based current-controlled voltage-source inverter is used as an APF. The control algorithm for the APF is based on the perfect harmonic cancellation method which provides a three-phase reference supply current in phase with its positive-sequence fundamental voltage. The proposed APF is integrated into the model of a 90-kVA advanced aircraft electric power system under VSCF operation. The performance characteristics of the system are studied with the frequency of the generator's output voltage varied from 400 Hz to 800 Hz under different loading conditions.

This paper is organized as follows: the VSCF aircraft EPS model is described in Section II. The simulation results and characteristics of the system without APF are presented in Section III. In Section IV, a proposed shunt APF to improve power quality of the VSCF aircraft EPS is presented, while Section V presents the results and characteristics of the VSCF aircraft power system integrated with the shunt APF at the generator terminals, and conclusions are drawn in Section VI.

Manuscript received November 20, 2008. First published October 02, 2009; current version published December 23, 2009. Paper no. TPWRD-00873-2008.

A. Eid is with the Electrical Engineering Department, South Valley University, Aswan, Egypt. He is also with the University of Texas at Tyler, Tyler, TX 75799 USA (e-mail: ahmadeid@ieee.org).

H. El-Kishky is with the Electrical Engineering Department, The University of Texas at Tyler, Tyler, Texas 75799 USA (e-mail: helkishky@ sbcglobal.net).

M. Abdel-Salam is with the Electrical Engineering Department, Assiut University, Assiut 71518, Egypt (mazen2000m@yahoo.com).

T. El-Mohandes is with the Electrical Engineering Department, South Valley University, Aswan 81542, Egypt (tharwatm@yahoo.com).

Digital Object Identifier 10.1109/TPWRD.2009.2031672

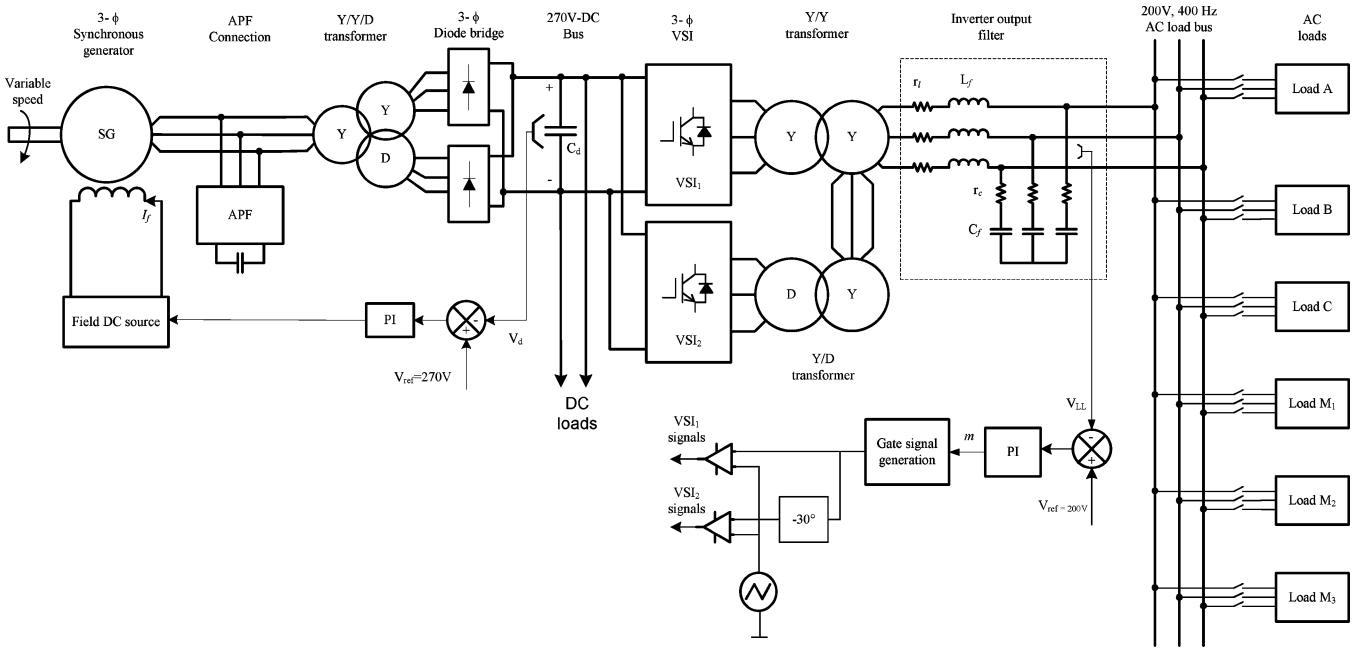

Fig. 1. Modeled VSCF aircraft electric power system with the APF, inverter passive filter, main loads, and controllers.

II. Structure and Modeling of the VSCF Aircraft Electric Power System

A. Generating System

The Boeing 767 aircraft electric power system consists of two independent channels, according to the number of starters/generators in the aircraft and an auxiliary/emergency power unit (APU) that contains an additional auxiliary starter/generator to provide power engines starting as well as for emergency backup. The generating system is comprised of starter/generators, power control units, and a generator and system control unit. A single channel of the aircraft electric system is studied here and shown schematically in Fig. 1.

Although the rated frequency of the aircraft power system is 400 Hz, in a VSCF system, the engine speed changes at approximately a 1:2 ratio, resulting in the aircraft synchronous generator frequency changing in the range of 400 Hz to 800 Hz [7]–[9]. During starting mode, the constant frequency system provides power through the interface power converter to the electric machine which acts as a starter to the aircraft engine. In the generating mode, the variable-speed engine in the aircraft acts as the prime mover for the field-controlled synchronous generator, resulting in variable frequency output power at the generator's terminals. This power is then delivered via the interface converter (dc link) to the constant frequency (400-Hz) aircraft electric power distribution system.

The modeled aircraft power system is equivalent to the Boeing 767 electric power system with a generator output of 90-kVA per channel. In this model, different load combinations are studied, including passive and dynamic ac loads as well as various dc loads on the aircraft system. Nonlinear loads, including constant power, constant current, as well as constant voltage loads are also considered. Several case studies are presented, including nonlinear as well as passive and dynamic ac loads. The power-quality characteristics of the studied aircraft electric power system with the proposed active filter are shown to be in compliance with the most recent military aircraft electrical standards MIL-STD-704F [7] as well as with the IEEE-Std. 519 [10]. Due to power conversion units used to obtain dc voltage and regulated 200-VAC (line voltage) at the ac load terminals, harmonics are generated in supply (generator) voltage and current waveforms. To meet the military aircraft electrical standards MIL-STD-704F as well as the IEEE-Std. 519, a fully controlled shunt APF is designed and integrated into the aircraft electric power system. The modeled aircraft power system parameters are listed in Table V while the governing equations of the aircraft generating system are presented in the Appendix.

B. Rectifier Unit

In order to eliminate the low-frequency output current harmonics of the synchronous generator, a transformer rectifier unit (TRU) with a passive 12-pulse power converter [2], [11], [12] is used in this study. The TRU, connected to the three-phase generator as shown in Fig. 1, provides inherent high power factor and low harmonic distortion. The power factor can be as high as 0.99 with a total harmonic distortion (THD) of about 13% [2], [3]. Power diodes in the TRU are normally robust and with no switching required, it means significant reduction in losses and, hence, improved efficiency as well as significant improvement in power quality of the system with lower harmonic contents and voltage transients. The Y/Y/D transformer in the VSCF aircraft power system provides the necessary phase shift of 30 ° for the 12-pulse operation feeding into the main 270-VDC bus (Fig. 1).

A dc capacitor is connected at the output of the power converter to smooth out the dc voltage. As the speed of the aircraft engine varies in the 1:2 range, the output voltage of the synchronous generator varies in frequency as well as in magnitude.

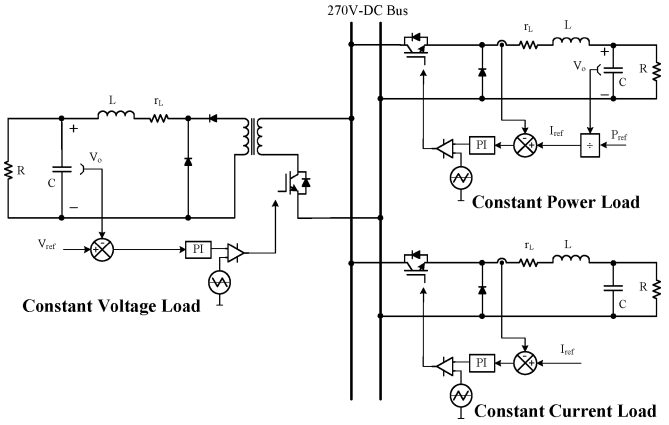

Fig. 2. Various controlled dc loads connected to the 270-VDC bus in the VSCF aircraft power system.

In turn, the 270-V dc bus is regulated by controlling the field current of the synchronous generator by using a feedback proportional-integral (PI) controller to meet the aircraft electrical standards [7]. The 100-kVA three-winding transformer (Fig. 1) has a 4% leakage inductance, a magnetizing current of 1%, and an X/R ratio of 3 with a full-load voltage regulation of 3.2%. Modeling and characterization of the VSCF aircraft power system was accomplished with the PSIM6.0 software package [15] with postprocessing performed in MATLAB.

C. DC Loads

In the proposed VSCF aircraft electric power system model, three different types of dc loads totaling 35.6 kW are connected to the regulated 270-VDC bus through various dc–dc converters. All controlled dc loads employ the simplest type of dc-dc converter configurations in which only one switch is needed and, hence, significantly minimizing switching losses. These loads are classified as constant power (CP) loads, constant current (CC) loads, and constant voltage (CV) loads, as shown in Fig. 2. The dc loads are distributed throughout the aircraft and used for various purposes, including heating services, actuation, subsystem controllers, and avionic systems [3].

The constant power load is connected to the main dc bus through a dc–dc buck converter where the load power is kept constant at 10 kW via controlling the sensing inductor current using a PI controller. The reference current is calculated by dividing the input reference power by the sensor output voltage. The PI controller modulates the error signal which is then compared to a sawtooth signal to generate a gate signal for the switch. Similarly, the CC load is obtained by using a controlled dc–dc buck converter. The load current is regulated and set at 100 A by using a PI controller with a resulting load voltage of 200 V and, hence, 20-kW load power.

On the other hand, the constant voltage load is regulated to have an output voltage value of 28 VDC which is used for the battery system and other constant voltage dc loads in the aircraft system. A forward power converter is used to reduce the 270-V DC voltage level to a suitable controlled voltage by using a high-frequency transformer. At steady state, the load will draw approximately 200 A with a load power of approximately 5.6 kW.

D. Power Inverter

The rms output voltage of a sinusoidal PWM inverter is given in terms of its input dc voltage V_d and the modulation index m [13] as

$$V_{ph} = 0.5 \times m \times \frac{V_d}{\sqrt{2}}. \tag{1}$$

For a rated rms output voltage per phase of 115 V and a modulation index of 1, the lowest required dc voltage V_d is 325 V. Therefore, a 12-pulse PWM inverter equipped with an output passive filter is used in the system (Fig. 1). Since the turns ratio of the D transformer is $\sqrt{3}$ times that of the Y-connected transformer and the pulse train of one converter is shifted by 30° with respect to the other, the combined output voltage would have a 12-pulse waveform, with a harmonic order given by

$$h = k\,p \pm 1, \quad V_h = \frac{V_1}{h}. \tag{2}$$

The THD of the voltage is given as

$$THD_v = \frac{\sqrt{\sum_{h=2}^{\infty} V_h^2}}{V_1} \tag{3}$$

where h is the characteristic harmonic order, k is a constant $(1, 2, \ldots)$, p is the converter pulse number, V_h is the harmonic voltage, and V_1 is the fundamental voltage.

To provide 115 V/200 V rms, 400 Hz at the main ac bus, and to further reduce the amount of harmonics injected into the supply, two six-pulse inverters are used and fed from the 270-VDC main bus. The inverters are directly connected to the primary windings of two separate three-phase transformers. In turn, the Y/Y and Y/D transformers are connected to the main ac bus to provide the 30° phase shift needed for a true 12-pulse inverter. The 12-pulse inverter is controlled by using a PI controller to provide a phase voltage of 115 V, 400 Hz at the main ac load bus. The voltage error signal is processed by the PI controller to provide the required modulation index m. Using the generated modulation index m, the appropriate gate signals are generated and fed to the twin six-pulse inverters.

E. AC Loads

Both passive and dynamic ac loads are considered in the modeled VSCF aircraft electric power system. Passive loads are simulated by using lumped circuit elements of series RL with a minimum load power factor of 0.85 lagging as recommended by aircraft electrical standards [7]. The ac loads are labeled A, B, and C and are shown schematically in Fig. 1. More details are presented in Table I. Furthermore, the dynamic loads are simulated with three induction motors labeled M_1, M_2, and M_3, respectively (Fig. 1). The selected motors are of ratings 11.2 kW, 7.5 kW, and 5.0 kW, respectively (Table I). The motors which commonly exist [14] on an aircraft for electro-hydro mechanical actuation are connected to the 115/200-V, 400-Hz main ac

TABLE I
AC LOADS PARAMETERS

Load	S (kVA)	R (Ω)	L (mH)	PF	I (A)
A	18.0	2.0	0.4	0.90	52.0
B	2.6	14.0	2.8	0.90	8.0
C	15.2	2.3	0.5	0.87	45.0
M_1	Load torque = 9 Nm				
M_2	Load torque = 6 Nm				
M_3	Load torque = 4 Nm				

TABLE II
LOAD CASE-STUDIES OF THE MODELED VSCF AIRCRAFT EPS.

Case-study No.	Passive loads	Dynamic loads	DC loads	% of full load
1			x	40%
2	x	x		65%
3	x	x	x	100%

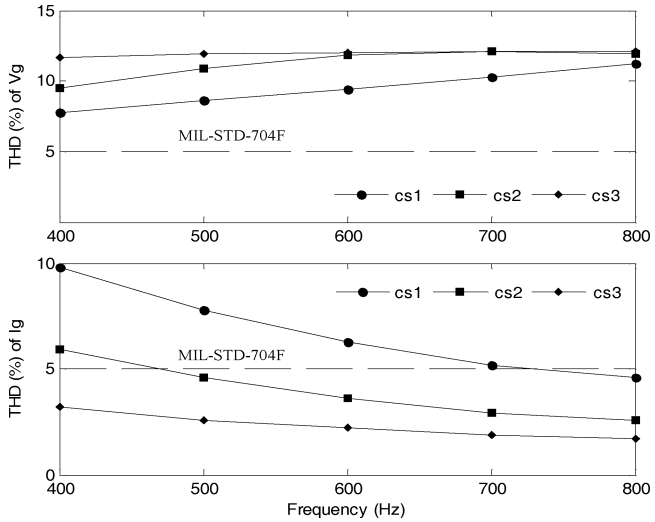

Fig. 3. Calculated THD values for Vg and Ig without APF.

bus. The motors are loaded with constant load torque and fed from the main ac load bus along with the passive ac loads.

III. PERFORMANCE CHARACTERISTICS OF THE VSCF AIRCRAFT EPS WITHOUT APF

The proposed model of the VSCF aircraft electric power system shown in Fig. 1 is developed and characterized by using the PSIM6 software package with postprocessing completed in MATLAB. In the model, the synchronous generator speed is controlled by using a speed governor to provide an output with a frequency range of 400 to 800 Hz with the systems nominal frequency set at 400 Hz. Different loading scenarios of the aircraft power system are presented in Table II with three case studies, including combinations of both ac and dc loads. The first case study dealing with various dc loads in the system, examines the effects of the 12-pulse passive rectifier on the system performance. With 35 kVA, the combined dc loads represent approximately 40% of the total power capacity per channel on the aircraft system. All passive (A, B, C) and dynamic (M_1, M_2, M_3) ac loads are combined and considered in case study 2, which represents slightly more than 60% of the total power capacity per channel on the aircraft system. The last case study investigates the VSCF aircraft power system characteristics under full-load condition with all ac and dc loads connected to the system.

In each case study, the current and voltage characteristics are generated and the THD values are calculated and compared to the established aircraft electrical standards.

Moreover, the rms value of the generator voltage (V_g) and current (I_g) as well as the ac load bus voltage (V_L) and current (I_L) are recorded. In case study 1, considering dc loads only with the dc power obtained by using a 12-pulse passive rectifier, the expected characteristic harmonics are given in (2). All power-quality characteristics of the VSCF aircraft system are generated over a 400- to 800-Hz frequency range of operation.

The simulation results of the first case-study (cs1) show interesting behavior of the harmonic contents in the generator voltage and current waveforms over the frequency range of operation as shown in Fig. 3. The THD value of the generator voltage can be more than 11% at 800-Hz operation, while the maximum THD value for the generator current is slightly less than 10% and occurs at 400 Hz. The THD values of the generator voltage increase with increasing frequency while the THD values for the generator current decrease with increasing the frequency of operation (Fig. 3), which may be attributed to the inductive nature of the system harmonic impedance. Due to the assumed balanced conditions of the load and source, the THD values remain consistent for all phases.

In case study 2 (cs2), only ac loads are connected to the modeled VSCF aircraft electric power system through a 12-pulse sinusoidal PWM inverter (Fig. 1), the calculated THD values are comparable to those obtained in cs1 while maintaining virtually the same trend of variation against frequency. With the full load applied in cs3, the THD in the generator voltage stays virtually leveled at approximately 12%. Further investigation of Fig. 3 shows that the THD values of the generator current I_g are significantly higher at lower loads (cs1) compared to those obtained at higher loads (cs2 and cs3).

This may be attributed to a lower fundamental component of the generator current I_{g1} at lighter loads which makes the THD value considerably higher than those obtained at higher loads.

At higher frequencies, the THD of the generator current falls to within the standard limit of 5% [7], [10], Fig. 3. The waveforms of the generator voltage Vg and current Ig are shown in Fig. 4 for cs3 with all combined ac and dc loads connected to the modeled VSCF aircraft electric power system at different frequencies. The calculated THD values of the generator current remain low and within the established standard limits over the entire frequency range of operation. However, the THD values of the generator voltage are significantly higher and remain virtually constant at 12% over the frequency range, which may be attributed to the inductive nature of the system harmonic impedance (Fig. 3). Moreover, Fig. 3 shows the THD of the current and voltage at the generator terminals compared to the maximum value of 5% as required by IEEE Std-519 and MIL-STD-704F.

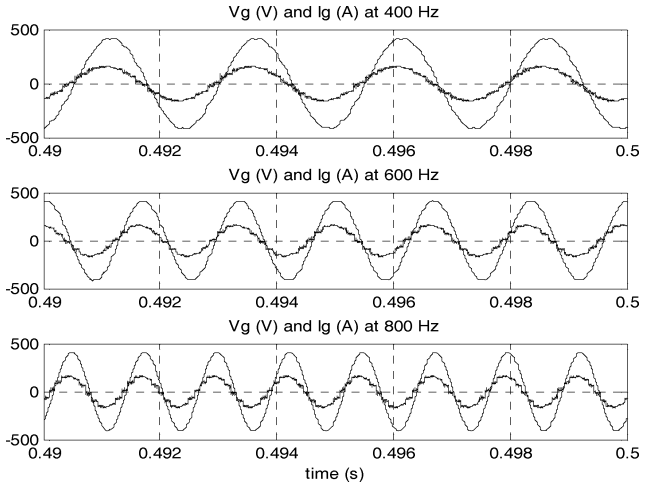

Fig. 4. Case study No. 3 generator voltage (Vg) and current (Ig) waveforms at different frequency operation.

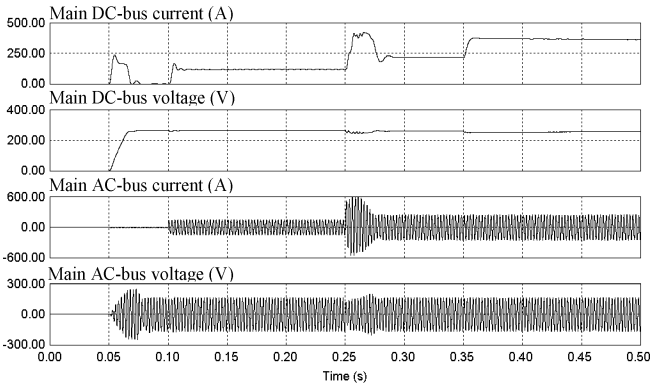

Fig. 5. Plot of the currents and voltages at the main dc and ac buses.

The waveforms showing transients in the main dc-bus current and voltage as well as in the main ac bus are presented in Fig. 5 with the timed load switching.

IV. Proposed APF Model and Control Strategy

A. Mathematical Modeling of APF

The APF, in general, is comprised of a power circuit, such as a voltage-source inverter (VSI), a smoothing inductors L_f with a series resistance r_f, and a dc capacitor $\mathrm{C_{dc}}$ as shown in Fig. 6. The capacitor connected to the dc bus of the VSI serves as an energy-storage element. Using simple network analysis, the performance of the APF model can be described with the governing differential (4) at the ac side [16]

$$\frac{d}{\mathrm{dt}}\left[i_{fn}\right] = -\frac{r_f}{L_f}\left[i_{fn}\right] + \frac{1}{L_f}\left[v_{sn} - v_{fn}\right] \tag{4}$$

where r_f and L_f are the series resistance and inductance per phase of the APF, i_{fn} is the APF phase current, while v_{fn} is the PWM phase voltages at the ac side and n takes a, b, c. The corresponding equation on the dc side can be given by [16]

$$C_{\mathrm{dc}}\frac{d}{\mathrm{dt}}V_{\mathrm{dc}} = i_{fa}\,SA + i_{fa}\,SB + i_{fa}\,SC \tag{5}$$

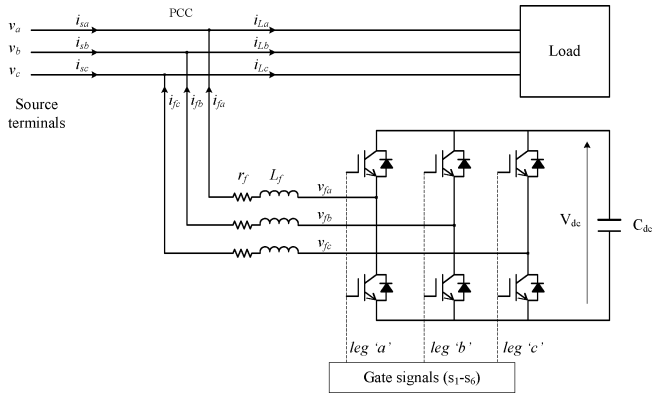

Fig. 6. APF configuration and connection.

where $\mathrm{C_{dc}}$ is the energy-storage capacitance connected to the dc side of the APF and $\mathrm{V_{dc}}$ is the available input dc voltage. The three-phase APF voltages can be expressed in terms of the dc voltage and the switching functions (SA, SB, and SC) according to the control circuit as given

$$\begin{bmatrix} v_{fa} \\ v_{fb} \\ v_{fc} \end{bmatrix} = \frac{1}{3}V_{\mathrm{dc}}\begin{bmatrix} 2\,SA - SB - SC \\ -SA + 2\,SB - SC \\ -SA - SB + 2\,SC \end{bmatrix}. \tag{6}$$

B. Control Method of the Proposed APF

Although the instantaneous reactive power theory (p-q theory) is widely used in the APF control circuitry to calculate the desired compensation current [17]–[22], it is very sensitive to distortion and imbalance that may occur in the voltage at the point of common coupling (PCC). On the other hand, the unity power factor control method [23], [24] does not work well in the presence of zero-sequence voltage components. Similar to the p-q control strategy, the i_d-i_q control method [25], [26] is sensitive to distortion and to imbalance. For full compliance with the respective harmonics standards, imbalance elimination, and reactive power compensation, the perfect harmonic cancellation (PHC) method [22], [23] is the control strategy of choice that is capable of corrective action under all conditions. This, in turn, is achieved through a two-stage procedure. First, the reference filter currents ($\mathrm{i_{far}}$, $\mathrm{i_{fbr}}$, and $\mathrm{i_{fcr}}$) are obtained and in the second stage, a PWM hysteresis band current control is used to generate the required gate signals ($\mathrm{s_1}$-$\mathrm{s_6}$) which are then fed to the inverter switches.

The PHC control method is adopted here to generate the required compensation currents for the shunt active power filter. The governing equations of the PHC control method can be derived [22]–[27]. Any set of voltages (v_{a}, v_{b}, v_{c}) and currents (i_{a}, i_{b}, i_{c}) can be transformed into the α-β-0 system where T is the transformation matrix using the power invariant as

$$\begin{bmatrix} v_o \\ v_\alpha \\ v_\beta \end{bmatrix} = T\begin{bmatrix} v_{\mathrm{a}} \\ v_{\mathrm{b}} \\ v_{\mathrm{c}} \end{bmatrix}, \begin{bmatrix} i_o \\ i_\alpha \\ i_\beta \end{bmatrix} = T\begin{bmatrix} i_{\mathrm{a}} \\ i_{\mathrm{b}} \\ i_{\mathrm{c}} \end{bmatrix}. \tag{7}$$

The function of the APF, controlled with the PHC method, is to compensate for all of the harmonic currents, provide the fundamental reactive power demanded by the load, and eliminate imbalance if it exists. To achieve these objectives altogether, the source current must be in phase with the fundamental positive-sequence component of the voltage at PCC [23]. Therefore, the reference source current can be given in the form

$$i_{sr} = K \cdot v_1^+ \tag{8}$$

where v_1^+ is the PCC voltage positive-sequence component.

The power delivered by the source p_s will be

$$p_s = v \cdot i_{sr} = v \cdot K \cdot v_1^+. \tag{9}$$

The constant K can be determined by using the condition that the source power is equal to the average power (active power) $\bar{P}_L$ demanded by the load, thus

$$K = \frac{\bar{p}_L}{(v_{\alpha 1}^{+2} + v_{\beta 1}^{+2})}. \tag{10}$$

The reference source current will then be given by [27]

$$\begin{bmatrix} i_{s0r} \\ i_{s\alpha r} \\ i_{s\beta r} \end{bmatrix} = K \begin{bmatrix} 0 \\ v_{\alpha 1} \\ v_{\beta 1} \end{bmatrix} = \frac{\bar{p}_L}{v_{\alpha 1}^{+2} + v_{\beta 1}^{+2}} \begin{bmatrix} 0 \\ v_{\alpha 1}^{+} \\ v_{\beta 1}^{+} \end{bmatrix}. \tag{11}$$

After converting the α-β-0 components to the a-b-c phase quantities, the APF reference currents are generated as [27]

$$[i_{fnr}] = [i_{Ln}] - [i_{snr}]. \tag{12}$$

Complete details of the PHC control method steps as calculated in the simulation program are shown in Fig. 7. A hysteresis band PWM current control scheme is applied in this study to control the inverter so that its output current follows the reference current waveform [27], [28]. In this method, the switches in an inverter are asynchronously controlled and the actual current is ramped up and down to follow the reference current. When the actual current exceeds the upper limit or drops below the lower hysteresis limit, the associated switching pattern of the switch will force the current to get back within the hysteresis band limit. Hence, the current ramp can be altered by the width of the hysteresis band. Decreasing the hysteresis band results in the filter current by following exactly the filter reference current; however, it increases switching losses.

V. Performance Characteristics of the VSCF Aircraft EPS With APF

The VSCF aircraft electric power system model with the proposed fully controlled active power filter is developed and studied under steady-state conditions. A three-phase current-controlled VSI inverter is used as an APF. The control algorithm for the APF is based on the perfect harmonic cancellation method which provides a three-phase reference supply current in phase with its positive-sequence fundamental voltage. The PHC control method will maintain the PF of the generator at or near unity. At the 115-V/200-V main ac load bus, a sinusoidal PWM 12-pulse inverter transforms the dc voltage into ac to feed all ac loads connected to the aircraft EPS.

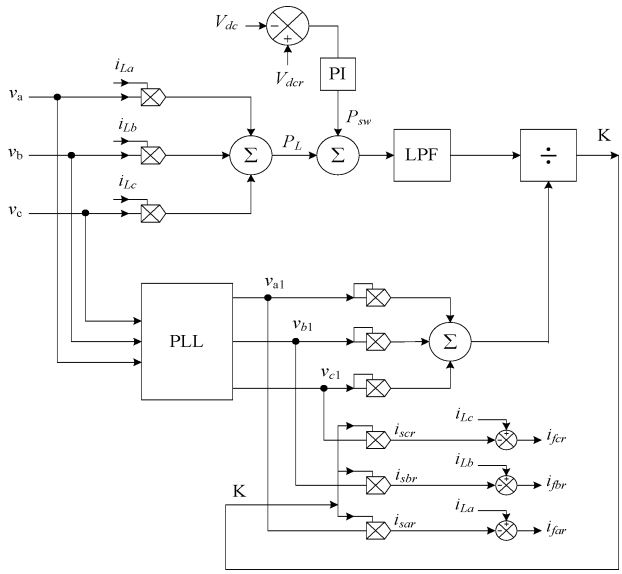

Fig. 7. APF control circuit configuration using the PHC method.

TABLE III
Design Parameters of the Proposed APF

Source line voltage	200	V
Source frequency	400-800	Hz
Filter inductor, L_f	0.1	mH
Series inductor resistance	0.01	Ω
Filter DC capacitor, C_{dc}	1.5	mF
DC reference voltage, V_{dcr}	600	V
Hysteresis band, hb	0.01	A
PI gain	200	A
PI time constant	1	s

The inverter output filter (see Fig. 1) mitigates the generated harmonics of the PWM inversion, and the inductive nature of the ac loads helps mitigate current harmonics along with the passive filter. The inverter output filter consists of a series inductor along with a shunt capacitor each having a small series resistance (Fig. 1). The design parameters of the inverter output filter are given in Table III with the series inductor value L_f selected at 0.1 mH with a series resistance r_l of 10-mΩ and the shunt connected capacitor C_f has a set value of 0.2 mF and a resistance r_c of 20 mΩ. A complete list of the APF design parameters is presented in Table III.

The proposed APF is integrated into the model of a 90-kVA advanced aircraft electric power system under variable-speed constant-frequency operation. The performance characteristics of the VSCF aircraft system power quality are studied with the frequency of the generator's output voltage varied from 400 to 800 Hz under different loading conditions. Several case studies are presented including dc loads as well as static and dynamic ac loads.

The THD values of the generator voltage and current are calculated for the same case studies (cs1-cs3) with different loading scenarios with the APF installed at the generator terminals and

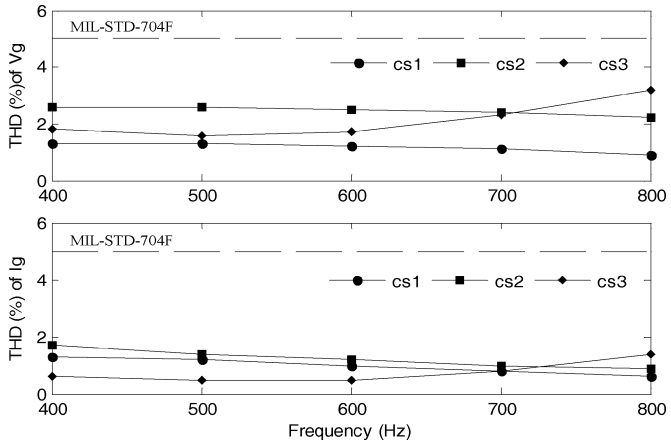

Fig. 8. Generator voltage and current THD for the three studied cases when installing the APF at the generator terminals.

TABLE IV
REDUCTION IN THD VALUES OF THE GENERATOR VOLTAGE AND CURRENT WITH APF

Frequency (Hz)	Reduction in THD of Vg			Reduction in THD of Ig		
	cs1	cs2	cs3	cs1	cs2	cs3
400	83.3%	72.6%	84.6%	86.7%	71.2%	80.6%
500	85.1%	76.4%	86.9%	85.1%	69.0%	82.7%
600	87.2%	78.8%	85.8%	84.1%	66.7%	75.9%
700	89.5%	80.4%	81.4%	84.4%	64.7%	55.2%
800	92.0%	81.5%	73.6%	87.0%	64.2%	17.6%

plotted in Fig. 8. Comparing Figs. 3 and 8, one can see a significant drop in harmonic contents in the generator voltage and current waveforms over the frequency range of operation.

The voltage-stiff nonlinear load of the diode rectifier unit with a large capacitive filter at the dc link feeding the VSI inverters results in nonsinusoidal currents and significant distortions of the ac terminal voltage. The voltage-source loads connected to the main ac bus draw discontinuous and nonsinusoidal currents with high THD and contribute to high THD, low-power factor, and distortion of ac voltage.

A measure of the harmonic compensation effectiveness of the proposed APF is presented in Table IV. The percentage drop of the THD values of the generator voltage and current after installing the APF over the frequency range of operation are presented. The recorded drop in the generator current's THD ranges from slightly less than 18% to 87%, while a range of drop of 72% to 92% was achieved in the voltage THD. It is important to point to the fact that the inductive nature of the system harmonic impedance of the modeled VSCF aircraft EPS considerably contributed to lowering the current harmonic contents and particularly at higher frequencies. Generally, the APF's effective harmonic compensation and the overall improvement in power quality of the VSCF aircraft EPS may be attributed to the effective PHC control scheme of the proposed fast-switching, real-time APF.

In case study 3 (full load), the load current i_{La}, the generator current i_{ga}, and the APF phase current i_{fa} (see Fig. 6) are shown in Fig. 9. The generator waveforms of phase voltage and current

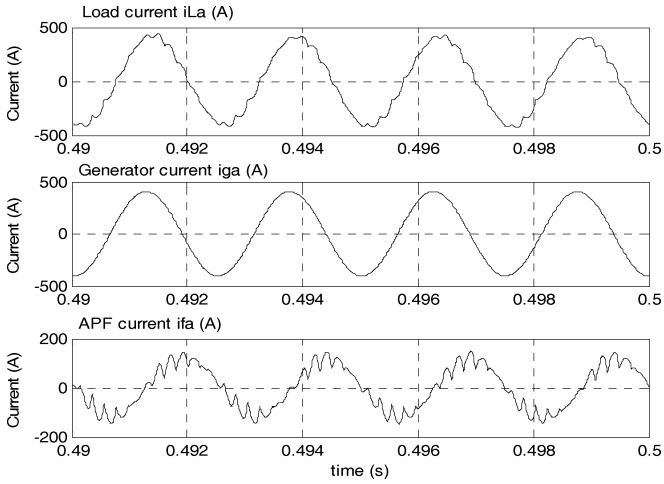

Fig. 9. Load current i_{La}, the generator current i_{ga}, and the APF current i_{fa} for phase a.

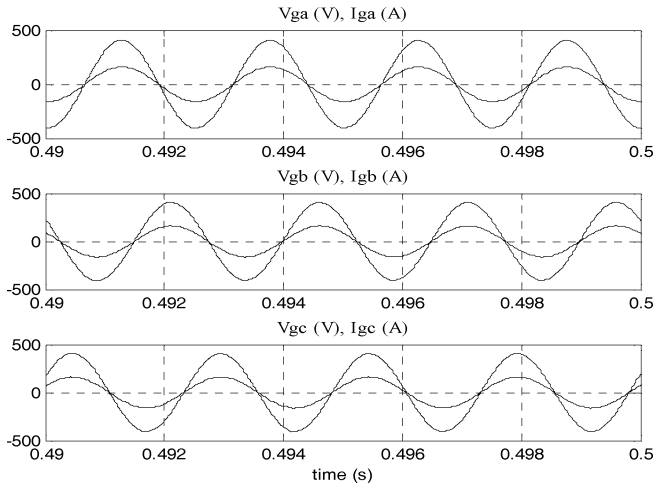

Fig. 10. Generator voltage and current for phase a, b and c at full load.

are shown in Fig. 10. With the PHC control method of the connected active filter, the generator's PF is maintained near unity which can be seen from the virtually zero phase shift between the generator voltage and current in Fig. 10. The change of the generator's PF with and without the shunt APF over the entire frequency range of operation from 400 to 800 Hz is presented in Fig. 11. The effect of the APF in correcting the generator's PF is obvious.

The transient voltage characteristics of the modeled VSCF aircraft EPS are presented in Figs. 12 and 13. Passive ac loads are switched to the aircraft system after 100 ms (allowing enough time for the generator voltage to reach steady state), followed by dynamic ac loads which are switched to the system after 250 ms, and then the nonlinear dc loads are switched on after 350 ms. Fig. 12 shows the generator phase voltage profile at 400, 600, and 600 Hz. Further investigation of Fig. 12 shows that the generator voltage transients are more significant toward the high end of the frequency range of operation; however, the transient magnitude and time duration are still within the strict requirements of the aircraft military standards. Fig. 13 shows the voltage transients at the main 270-VDC bus in response

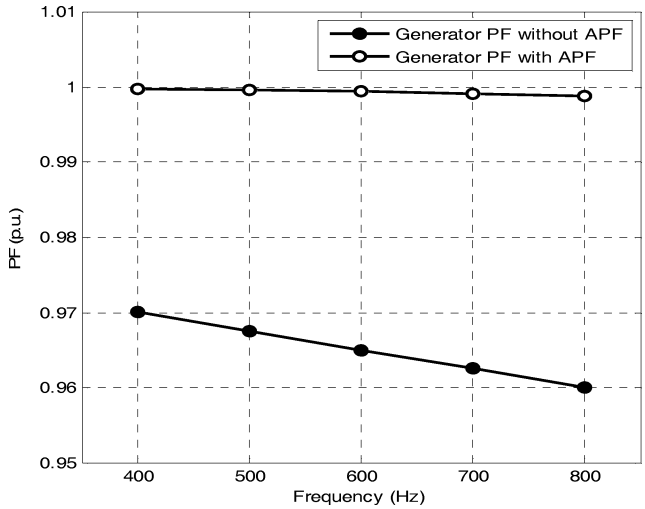

Fig. 11. Generator's PF with and without the APF installed.

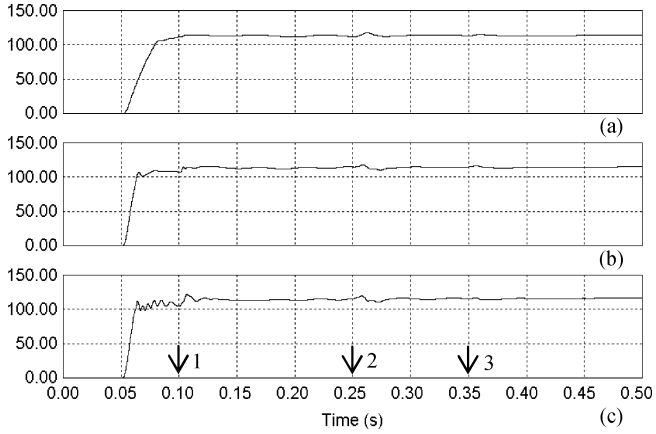

Fig. 12. Transients in the generator phase voltage (V) at an operating frequency of (a) 400 Hz, (b) 600 Hz, and (c) 800 Hz.

to timed load switching. Despite the pronounced presence of the main dc-bus voltage transients along almost the entire frequency range of operation, the magnitude and time duration of the transients are within the limits of the applicable military standards. The steady-state dc voltage is smooth and fixed at 270 V by virtue of the dc capacitor C_d, Fig. 1. The dc cable used is 000AWG size with a resistance of 19-$\mu\Omega$/m and a series inductance of 0.1-μH/m. The average length of the cable considered for the B767 is 56 m.

Fig. 14 presents the generator's current transient characteristics at 400–, 600-, and 800-Hz operating frequency as the passive ac loads are switched on to the EPS at 100 ms, followed by the dynamic ac loads at 250 ms, and then the nonlinear dc loads at 350 ms.

To study the performance of the modeled VSCF aircraft electric power system under unbalanced conditions, an unbalanced three-phase load is switched on to the 115-V/200-V main ac bus at 400-Hz generator frequency. The load three-phase currents (175 A, 142 A, 121 A), the APF current, and the generator currents are all shown in Fig. 15. Further investigation of Fig. 15 shows that despite the significant unbalance of the load currents, the generator currents are perfectly balanced which is attributed

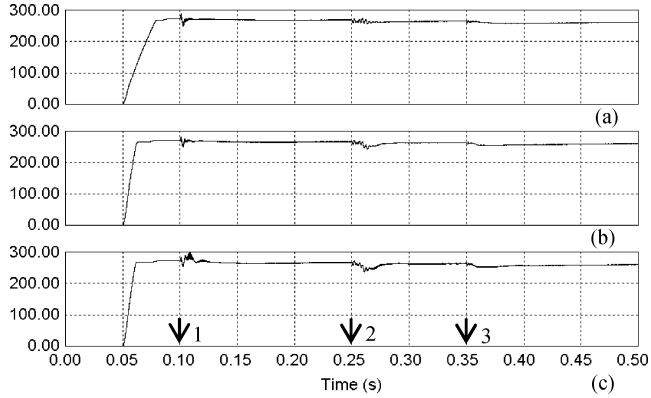

Fig. 13. Transients in the 270-VDC bus voltage (V) at an operating frequency of (a) 400 Hz, (b) 600 Hz, and (c) 800 Hz.

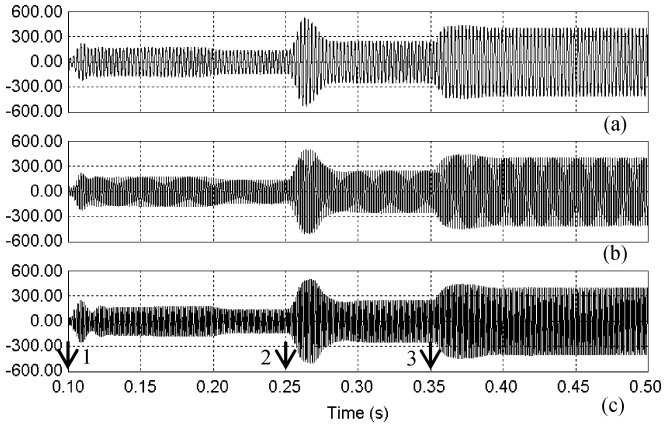

Fig. 14. Generator current transients with the switching of passive ac loads at an operating frequency of (a) 400 Hz, (b) 600 Hz, and (c) 800 Hz.

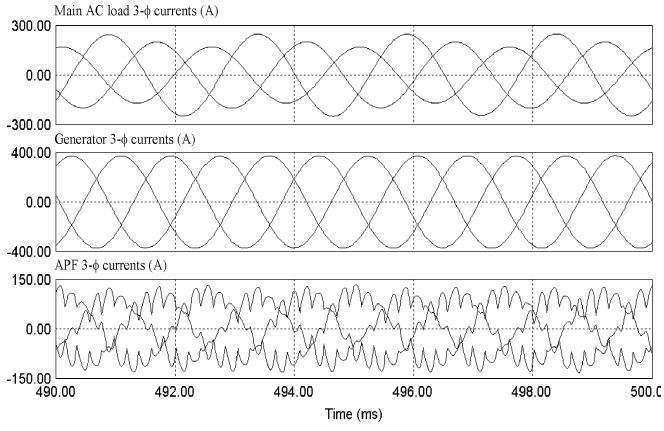

Fig. 15. Unbalanced ac load currents, generator currents, and the APF currents injected into the system.

to the real-time compensation by the fully controlled APF connected to the VSCF at the generators' terminals.

VI. Conclusion

A comprehensive model of the VSCF aircraft electric power system is developed to study the performance characteristics of the system. In particular, the power quality of the VSCF aircraft EPS is studied over a wide frequency range of 400 Hz to 800 Hz.

TABLE V
SYSTEM PARAMETERS AND CONSTANTS

Definition	Value
Synchronous generator parameters	
Stator winding resistance	0.01Ω
leakage inductance	18μH
d-axis magnetizing inductance	0.442mH
q-axis magnetizing inductance	0.411mH
Field winding resistance	0.012 Ω
Field winding leakage inductance	0.01mH
Rotor damping cage d-axis resistance	0.01 Ω
Rotor damping cage d-axis leakage inductance	50μH
Rotor damping cage q-axis resistance	0.01 Ω
Rotor damping cage q-axis leakage inductance	50μH
Number of Poles	4
Moment of inertia of the machine	0.01 kg*m^2
Cable parameters	
Resistance per meter	3.71mΩ/m
Inductance per meter	3.28nH/m
Capacitance per meter	3.28pF/m
PI controller parameters	
Proportional gain for 270VDC bus	1
Integral gain for 270VDC bus	10
Proportional gain for AC load bus	3.5x10^{-3}
Integral gain for AC load bus	3
28VDC bus smoothing filter parameters	
Inductance	0.1mH
Capacitance	1.2mF

A fully controlled APF is designed to regulate the load terminal voltage, eliminate harmonics, correct the supply power factor, and minimize the effect of unbalanced loads. The proposed APF is integrated into the model of the aircraft electric power system under variable-speed constant-frequency operation.

The performance characteristics of the system are studied with the frequency of the generator's output voltage varied from 400 Hz to 800 Hz under different loading conditions. Several cases studies are presented including dc loads as well as passive and dynamic ac loads. It is important to point to the fact that the inductive nature of the system harmonic impedance of the modeled VSCF aircraft EPS considerably contributed to lowering the current harmonic contents and particularly at higher frequencies. Generally, the effective harmonic compensation and the overall improvement in power quality of the modeled VSCF aircraft EPS may be attributed to the effective PHC control scheme of the proposed fast-switching, real-time APF. The power-quality characteristics of the studied VSCF aircraft electric power system with the proposed active filter are shown to be in compliance with the most recent military aircraft electrical standards MIL-STD-704F as well as with the popular IEEE-Std. 519.

APPENDIX
SYNCHRONOUS GENERATOR MODEL [29]

Stator equations

$$v_d = -R_s\, i_d - \omega\, \lambda_q - (L_{ls} + L_{md})\, \frac{di_d}{\mathrm{dt}} + L_{md}\, \frac{di_{fd}}{\mathrm{dt}} + L_{md}\, \frac{di_{kd}}{\mathrm{dt}}$$

$$v_q = -R_s\, i_q + \omega\, \lambda_d - (L_{ls} + L_{mq})\, \frac{di_q}{\mathrm{dt}} + L_{mq}\, \frac{di_{fd}}{\mathrm{dt}}.$$

where

$$\lambda_d = -(L_{ls} + L_{md})\, i_d + L_{md}\, (i_{fd} + i_{kd})$$

$$\lambda_q = -(L_{ls} + L_{mq})\, i_q + L_{mq}\, i_{kq}.$$

Field equation

$$v_{fd} = R_{fd}\, i_{fd} - L_{md}\frac{di_d}{\mathrm{dt}} + (L_{\mathrm{lfd}} + L_{md})\, \frac{di_{fd}}{\mathrm{dt}} + L_{md}\frac{di_{kd}}{\mathrm{dt}}.$$

Damper winding equations

$$0 = R_{kd} i_{kd} - L_{md}\frac{di_d}{\mathrm{dt}} + L_{md}\frac{di_{fd}}{\mathrm{dt}} + (L_{\mathrm{lkd}} + L_{md})\, \frac{di_{kd}}{\mathrm{dt}}$$

$$0 = R_{kq} i_{kq} - L_{mq}\frac{di_q}{\mathrm{dt}} + (L_{\mathrm{lkq}} + L_{mq})\, \frac{di_{kq}}{\mathrm{dt}}.$$

The parameters and variables (reflected to the stator) in the equations just shown have the following meanings: ω is the rotor speed; v_d, i_d, and v_q, i_q are the armature d- and q-axis terminal voltages and currents, respectively; and v_{fd} and i_{fd} are the field winding terminal voltage and current. i_{kd} and i_{kq} are the d- and q-axis damper winding currents. λ_d and λ_q are the total armature flux in the d- and q-axis. R_s and L_{ls} are the armature phase resistance and leakage inductance. L_{md} and L_{mq} are the d- and q-axis coupling inductance. R_{fd} and $\mathrm{L}_{\mathrm{lfd}}$ are the field winding resistance and leakage inductance. R_{kd}, R_{kq}, $\mathrm{L}_{\mathrm{lkd}}$, and $\mathrm{L}_{\mathrm{lkq}}$ are the d- and q-axis damper.

REFERENCES

[1] J. A. Rosero, J. A. Ortega, E. Aldabas, and L. Romeral, "Moving towards a more electric aircraft," *IEEE Aerosp. Electron. Syst. Mag.*, vol. 22, no. 3, pp. 3–9, Mar. 2007.

[2] K. W. E. Cheng, "Comparative study of AC/DC converters for more electric aircraft," in *Proc. Inst. Elect. Eng. Power Electronics and Variable Speed Drives Conf.*, 1998, pp. 299–304.

[3] A. Eid, M. Abdel-Salam, H. El-Kishky, and T. El-Mohandes, "Simulation and transient analysis of conventional and advanced aircraft electric power systems with harmonic mitigation," *Elect. Power Syst. Res.*, vol. 79, no. 4, pp. 660–668, Apr. 2009.

[4] V. V. Vadher, I. R. Smith, and S. Williams, "Mathematical modeling of a VSCF aircraft generating system," *IEEE Trans. Aerosp. Electron. Syst.*, vol. AES-22, no. 5, pp. 573–582, Sep. 1986.

[5] M. A. Rosswurm, "Design considerations of dc-link aircraft generation systems," in *Proc. Aerospace Congr. Expo.*, Anaheim, CA, 1981, pp. 1–15.

[6] D. S. Yorksie and W. E. Hyvarinen, "The effect of critical design parameters on the selection of a VSCF system," in *Proc. Aerospace Congr. Expo.*, Anaheim, CA, 1981, pp. 43–50.

[7] *"Aircraft Electric Power Characteristics", Military Standard*, MIL-STD-704F, 2004.

[8] T. M. Jahns and M. A. Maldonado, "A new resonant link aircraft power generating system," *IEEE Trans. Aerosp. Electron. Syst.*, vol. 29, no. 1, pp. 206–214, Jan. 1993.

[9] M. H. Taha, D. Skinner, S. Gami, M. Holme, and G. Raimondi, "Variable frequency to constant frequency converter (VFCFC) for aircraft applications," in *Proc. Inst. Elect. Eng. Int. Conf. Power Electronics, Machines and Drives*, Jun. 2002, pp. 235–240.

[10] *IEEE Recommended Practices and Requirements for Harmonic Control in Electrical Power System*, ANSI/IEEE Std. 519- 1992.

[11] G. Gong, U. Drofenik, and J. W. Kolar, "12-pulse rectifier for more electric aircraft applications," in *Proc. IEEE Int. Conf. Industrial Technology*, Dec. 2003, vol. 2, pp. 1096–1101.

[12] G. Guanghai, M. L. Heldwein, U. Drofenik, J. Minibock, K. Mino, and J. W. Kolar, "Comparative evaluation of three-phase high-power-factor AC-DC converter concepts for application in future more electric aircraft," *IEEE Trans. Industrial Electron.*, vol. 52, no. 3, pp. 727–737, Jun. 2005.

[13] B. K. Bose, *Modern Power Electronics and AC Drives*. Englewood Cliffs, NJ: Prentice-Hall., 2002.
[14] S. Chandrasekaran, D. K. Lindner, and D. Boroyevich, "Analysis of subsystem integration in aircraft power distribution systems," in *Proc. IEEE Int. Symp. Circuits and Systems*, 1999, vol. 5, pp. 82–85.
[15] Powersim, Inc. Woburn, MA. [Online]. Available: http://www.powersimtech.com
[16] B. Singh, K. AL-Haddad, and A. Chandra, "A new control approach to three-phase active filter for harmonics and reactive power compensation," *IEEE Trans. Power Syst.*, vol. 13, no. 1, pp. 133–138, Feb. 1998.
[17] H. Akagi, Y. Kanazawa, and A. Nabae, "Instantaneous reactive power compensators comprising switching devices without energy storage components," *IEEE Trans. Ind. Appl.*, vol. IA-20, no. 3, pp. 625–630, May/Jun. 1984.
[18] F.-Z. Peng, G. W. Ott, and D. J. Adams, "Harmonic and reactive power compensation based on the generalized instantaneous reactive power theory for three-phase four-wire systems," *IEEE Trans. Power Electron.*, vol. 13, no. 6, pp. 1174–1181, Nov. 1998.
[19] H. Akagi, S. Ogasawara, and H. Kim, "The theory of instantaneous power in three-phase four-wire systems: A comprehensive approach," in *Proc. IEEE IAS Annu. Meeting*, 1999, pp. 431–439.
[20] J. Afonso, C. Couto, and J. Martins, "Active filters with control based on the p-q theory," *IEEE Ind. Electron. Soc. Newslett.*, pp. 5–11, Sep. 2000.
[21] M. Aredes and E. H. Watanabe, "New control algorithms for series and shunt three-phase four-wire active power filters," *IEEE Trans. Power Del.*, vol. 11, no. 3, pp. 1649–1656, Jul. 1995.
[22] M. I. Montero, R. Cadaval, and F. B. Gonzalez, "Comparison of control strategies for shunt active power filters in three-phase four-wire systems," *IEEE Trans. Power Electron.*, vol. 22, no. 1, pp. 229–236, Jan. 2007.
[23] M.-R. Rafiei, H. A. Toliyat, R. Ghazi, and T. Gopalarathanam, "An optimal and flexible control strategy for active filtering and power factor correction under nonsinusoidal line voltages," *IEEE Trans. Power Del.*, vol. 16, no. 2, pp. 297–305, Apr. 2001.
[24] A. Cavallani and G. C. Montarani, "Compensation strategies for shunt-active filter control," *IEEE Trans. Power Electron.*, vol. 9, no. 6, pp. 587–593, Nov. 1994.
[25] A. Nabae and T. Tanaka, "A new definition of instantaneous active-reactive current and power based on instantaneous space vectors on polar coordinates in three phase circuits," *IEEE Trans. Power Del.*, vol. 11, no. 3, pp. 1238–1243, Jul. 1996.
[26] V. Soares, P. Verdelho, and G. D. Marques, "An instantaneous active and reactive current component method for active filters," *IEEE Trans. Power Electron.*, vol. 15, no. 4, pp. 660–669, Jul. 2000.
[27] A. Eid, M. Abdel-Salam, H. El-Kishky, and T. El-Mohandes, "Active power filters for harmonic cancellation in conventional and advanced aircraft electric power systems," *Elect. Power Syst. Res.*, vol. 79, no. 1, pp. 80–88, Jan. 2009.
[28] G. W. Chang, C.-M. Yeh, and W.-C. Chen, "Meeting IEEE-519 current harmonics and power factor constraints with a three-phase three-wire active power filter under distorted source voltages," *IEEE Trans. Power Del.*, vol. 21, no. 3, pp. 1648–1654, Jul. 1996.
[29] P. C. Krause, *Analysis of Electric Machinery*. New York: McGraw-Hill, 1987.

Ahmad Eid (S'06) was born in Qena, Egypt. He received the B.Sc. and M.Sc. degrees in electrical engineering from Assiut University, Assiut, Egypt, in 1997 and 2002, respectively, and is currently pursuing the Ph.D. degree in electrical engineering at the University of Texas at Tyler.

Currently, he is with the Electrical Engineering Department, South Valley University, Aswan, Egypt. He was a Research Engineer at the Malaya University, Kuala Lumpur, Malaysia, from 2003 to 2005 on a linear machine design project and with Kyungnam University, South Korea, in 2006 on a wind power generation project. His research activities include power quality of power systems, renewable energy sources, wind power, electrostatic filtering, and linear machines.

Hassan El-kishky (SM'04) received the B.Sc. degree in electric power systems and rotating machines from Ain Shams University, Cairo, Egypt, in 1984 and the M.Sc. and Ph.D. degrees in electrical engineering from Assiut University, Assiut, Egypt, and Arizona State University, Tempe, AZ, in 1990 and 1995, respectively.

Currently, he is an Associate Professor of Electrical Engineering at the University of Texas, Tyler. He is also a Consultant in the broad areas of electric power systems and electromagnetic interference/electromagnetic compatibility (EMI/EMC) and a Co-Founder of the National Energy Technologies, LLC, providing services in the design and analysis of electrical systems. He was the R&D Manager at the National Electric Coil from 1997 to 1998. His areas of interest include high-voltage insulation systems for large rotating machines, stress grading, and corona-suppression systems, modeling of the high-voltage phenomena, power quality of electric power systems, as well as electromagnetic interference and compatibility.

Dr. El-Kishky is a registered professional engineer in the State of Texas. He is also a certified EMC engineer by iNARTE.

Mazen Abdel-Salam (SM'78–F'93) was born in El-Monofia, Egypt. He received the B.Sc., M.Sc., and Ph.D. degrees in electrical engineering from the University of Cairo, Cairo, Egypt, in 1967, 1970, and 1973, respectively.

In 1967, he joined the Academy of Science and Technology, Cairo, as a Research Assistant. In 1973, he joined the Faculty of Electrical Engineering, Assuit University, Assuit, Egypt, as an Assistant Professor. He became an Associate Professor in 1977. During the academic years 1977–1979, he was an Alexander von Humboldt Fellow in the Electrical Engineering Department, Technical University of Munich, Munich, Germany, and was with the Electrical Engineering Department, University of Liverpool, Liverpool, U.K. In 1979, he joined the General Electric Co., Pittsfield, MA, as a Researcher. In 1982, he rejoined Assuit University as a Professor of Electrical Power Engineering. During the academic years 1984–1994, he was a Professor of Electric Power Engineering in the Department of Electrical Engineering, King Fahd University of Petroleum and Minerals, Dhahran, Saudi Arabia. He obtained Research Fellowships at the Military Technical University of Hamburg, Germany, in 1984; the University of Leeds, U.K., in 1988; and Kaiserlautern University, Germany, in 1989; Michigan Technological University, Houghton, in 1990; Toyohashi University, Japan, in 1995; the Technical University of Hamburg, Germany, in 1996; the University of Manchester, Manchester, U.K., in 2004 and 2005; and Toyohashi University of Technology, Japan, in 2006. He was the Chairman of the Electrical Engineering Department from 1996 to 2002 and Vice Dean for Student Affairs during 2002–2006 with the Faculty of Engineering, Assuit University. His research activities include corona studies, digital calculation of electric fields, investigations of high-voltage phenomena, low-voltage distribution networks, control of electrical machines, and renewable energy, including wind and PV systems and aircraft power systems. He is the author of *High Voltage Engineering–Theory and Practice* (Marcel Dekker, 2000). He taught several short courses in the areas of pollution control, high-voltage engineering, and power system protection and the design and diagnosis of power transformers for engineers from industrial firms and electric utilities in Egypt, Saudi Arabia, and Malaysia. He conducted several consultations and worked on some design projects in Egypt, Emirates, and Saudi Arabia.

Dr. Abdel-Salam was the Founder/Organizer of the Middle East Power System Conference (MEPCON) that was held in Egypt in 1989 and continued over the years. He is a member of the Electrostatic Processes Committee of the IEEE Industrial Applications Society. He received the Egyptian National Prize in 1986 and 1992, Excellence Prize in Electrical Power Engineering in 1997, Japanese Government Research Award for Foreign Specialists in 1999, National Prize in Scientific Distinction in 2000, National Prize in Scientific Creativity in 2001, National Appreciation prize in Engineering Sciences in 2004, SCOPUS award (from Elsevier) in 2008, and the Assiut University Prize for Scientific Excellence in 1999 and 2005 for contributions to high-voltage applications in industry. He became a Fellow of the Institution of Electrical Engineers, U.K., in 1992; Alexander-von-Humboldt Fellow, Germany, in 1977; Fellow of the Institute of Physics, U.K., in 2002; and Fellow of the Japanese Society for the promotion of Science, Japan, in 1996.

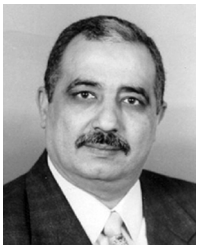

Mohamed T. El-Mohandes (M'89) was born in Egypt on March 3, 1952. He received the B.Sc. degree in electrical engineering, the M.Sc. degree in electrical power systems engineering, and the Ph.D. degree in high voltage engineering from Assiut University, Assiut, Egypt, in 1975, 1979, and 1986, respectively.

He was a Lecturer in the Electrical Engineering Department, Assiut University, Assiut, Egypt. He was the Dean of the Faculty of Engineering, South Valley University, Aswan, Egypt. Currently, he is the Vice President for undergraduate affairs at South Valley University, Aswan. His current research interests include corona studies and digital calculation of electric fields.

Dr. El-Mohandes has been on the Organizing Committee of the Middle East Power System Conference (MEPCON) since 1989.